AIAA 81-4239

Optimal Feedback Slewing of Flexible Spacecraft

John A. Breakwell*
Lockheed Missiles & Space Company, Inc., Palo Alto, Calif.

A method is presented for maneuvering a flexible spacecraft from one position to another while leaving an arbitrary number of bending modes inactive at the end of the maneuver. The method combines standard fixed-time linear quadratic Gaussian regulator control theory with a modal decomposition of a flexible body. Further features of the method are that it uses minimum control effort and it can be converted to a feedback form to deal with random disturbances and parameter uncertainties. Several examples are given to demonstrate the efficacy of the method, and results from a hardware experiment are presented.

I. Introduction

UNTIL recently, the maneuvers of flexible spacecraft have been performed relatively slowly to keep bending deformations small.

In this paper, we describe a numerical procedure for generating a feedback law that will maneuver a vehicle from one attitude to another, leaving any number of bending modes unexcited at the end of the maneuver. The time required to accomplish the maneuver is not restricted; an example is given of a half-second maneuver which leaves a 1 Hz bending mode unexcited at the end of the maneuver. To deal with parameter uncertainty and random disturbances, a means of converting an open-loop optimal maneuver to a feedback maneuver is shown. Because the gains used in the feedback scheme change with time, computer memory will have to be set aside to store them. (With proper manipulation however, a single set of gains may be used to perform any maneuver.)

We develop the theory which allows determination of open-loop control profiles to effect desired maneuvers. The basis of the theory is the fixed-time, linear, quadratic-loss minimization problem which is common in modern control theory. Starting with the Euler-Lagrange equations of this problem, the desired control profile is expressed in terms of a transition matrix. A model in state vector form is then described which represents a large class of flexible spacecraft. As an example, the transition matrix is used to generate open-loop control profiles, and computer simulations of two resulting slew maneuvers are presented.

In the case of such simple models, it is easy to obtain transition matrices analytically. However, as more bending modes are included in the model, it quickly becomes impossible to analytically derive the necessary transition matrices. Thus, a method for numerically developing the requisite transition matrices is presented next. This method is used to generate a control profile for a model including two bending modes. This control profile is put into a computer simulation, and a slew maneuver is generated. At the end of the maneuver, the first two bending modes are quiescent.

Section III of this paper shows how to convert open-loop control profiles into a feedback maneuvering law. Scaling laws which allow a single set of gains to be used for any maneuver are developed, and the sensitivity of the scheme to modeling errors is determined.

Finally, results from a hardware experiment are presented in Sec. IV.

II. Open-Loop Control Method

The control methods which are the subject of this paper are derived from the quadratic-loss minimization problem of modern control theory. The problem of the optimal slew maneuver can be mathematically stated as minimizing the quadratic cost function in Eq. (1), by choice of the control u subject to the constraints in Eq. (2), and the boundary conditions in Eq. (3).

$$\int_0^{t_f} (x^T A x + u^T B u)\,dt \tag{1}$$

$$\dot{x} = Fx + Gu \tag{2}$$

$$x(0) \quad \text{given} \quad x(t_f) = 0 \tag{3}$$

where x is the state vector, u is the control vector, and F and G are constant matrices which define the dynamical relation between u and x. A and B are positive definite weighting matrices on the state and control vectors, respectively.

Before relating these vectors and matrices to a flexible space vehicle, we will continue to solve the mathematical problem. The transformation of this calculus of variation problems into the Euler-Lagrange differential equations is covered in many textbooks, for instance, Chap. 5 of Bryson and Ho.[1] Here the Euler-Lagrange equations are

$$\begin{bmatrix} \dot{x} \\ \dot{\lambda} \end{bmatrix} = \begin{bmatrix} F & -GB^{-1}G^T \\ -A & -F^T \end{bmatrix} \begin{bmatrix} x \\ \lambda \end{bmatrix} \tag{4}$$

$$u = -B^{-1}G^T\lambda \tag{5}$$

$$x(0) \quad \text{given} \quad x(t_f) = 0 \tag{6}$$

The vector λ appearing in Eqs. (4) and (5) is called the costate, Lagrange multiplier, or adjoint vector. It appears in the process of converting the problem of Eqs. (1-3) into that given by Eqs. (4-6).

The solution to the system, Eq. (4), may be expressed in terms of a transition matrix as

$$\begin{bmatrix} x(t) \\ \lambda(t) \end{bmatrix} = \begin{bmatrix} \Phi_{11}(t) & \Phi_{12}(t) \\ \Phi_{21}(t) & \Phi_{22}(t) \end{bmatrix} \begin{bmatrix} x(0) \\ \lambda(0) \end{bmatrix} \tag{7}$$

Then, using the boundary conditions in Eq. (6), it follows that

$$x(t_f) = 0 = \Phi_{11}(t_f)x(0) + \Phi_{12}(t_f)\lambda(0) \tag{8a}$$

so

$$\lambda(0) = -\Phi_{12}^{-1}(t_f)\Phi_{11}(t_f)x(0) \tag{8b}$$

and, using Eq. (5) and the bottom of Eq. (7),

$$u(t) = -B^{-1}G^T[\Phi_{21}(t) - \Phi_{22}(t)\Phi_{12}^{-1}(t_f)\Phi_{11}(t_f)]x(0) \tag{9}$$

Received July 23, 1979; revision received Dec. 29, 1980.

*Senior Dynamics Engineer, Advanced Systems Division.

Equation (9) expresses the control vector u which takes the state vector from $x(0)$ at time zero to zero at time t_f while minimizing the cost function, Eq. (1).

Here are some examples illustrating the application of this mathematical theory to the maneuvering of spacecraft. Figure 1 shows a representation of a simple spacecraft. The spacecraft comprises two beams clamped symmetrically to a rigid central body. The maneuver to be performed is a rotation through an angle θ in the plane of the figure. This maneuver is to be performed in the time interval zero to t_f. The control to be used to effect the maneuver is torque T, perpendicular to this plane, applied to the rigid central body. In terms of system, or free-free modes, the dynamical equations are

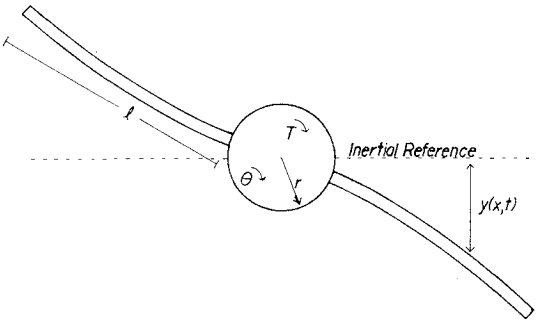

Fig. 1 Example specimen: J = total inertia = 4103.2 slug-in.^{2}; beam parameters adjusted to give $\omega_1 = 1.0$ Hz, $\omega_2 = 6.3$ Hz, $\omega_3 = 17.6$ Hz.

$$\frac{\mathrm{d}}{\mathrm{d}t}\begin{bmatrix} q_0 \\ \dot{q}_0 \\ \hline q_1 \\ \dot{q}_1 \\ \hline q_2 \\ \dot{q}_2 \\ \cdot \\ \cdot \\ \cdot \end{bmatrix} = \left[\begin{array}{cc:cc:cc:c} 0 & 1 & 0 & 0 & 0 & 0 & \cdots \\ 0 & 0 & 0 & 0 & 0 & 0 & \cdots \\ \hdashline 0 & 0 & 0 & 1 & 0 & 0 & \cdots \\ 0 & 0 & -\omega_1^2 & -2w_1\zeta_1 & 0 & 0 & \cdots \\ \hdashline 0 & 0 & 0 & 0 & 0 & 1 & \cdots \\ 0 & 0 & 0 & 0 & -\omega_2^2 & -2w_2\zeta_2 & \cdots \\ \hdashline \cdot & \cdot & \cdot & \cdot & \cdot & \cdot & \\ \cdot & \cdot & \cdot & \cdot & \cdot & \cdot & \\ \cdot & \cdot & \cdot & \cdot & \cdot & \cdot & \end{array}\right] * \begin{bmatrix} q_0 \\ \dot{q}_0 \\ \hline q_1 \\ \dot{q}_1 \\ \hline q_2 \\ \dot{q}_2 \\ \cdot \\ \cdot \\ \cdot \end{bmatrix} + \begin{bmatrix} 0 \\ 1/J \\ \hline \beta \\ \eta_1 \\ \hline 0 \\ \eta_2 \\ \cdot \\ \cdot \\ \cdot \end{bmatrix} T \tag{10}$$

In this description, q_0 is the "rigid-body" modal amplitude, and describes the way the spacecraft would turn if there were no flexing in the beams. The q_i are generalized modal amplitudes; the displacement of any point on the beams from an inertial reference is given by the infinite sum

$$y(x,t) = \sum_{i=0}^{\infty} q_i(t)\phi_i(x) \tag{11}$$

It follows from Eq. (10) that J must be the total inertia of the vehicle; the η_i are the influence coefficients of torque T on each modal amplitude q_i; and ζ_i are the modal damping coefficients.

In the first example, it is desired to move θ from θ_0 to zero in the time interval zero to t_f, leaving the first bending modal coordinate q_1 and its rate $\dot{q}_1$ equal to zero at the end of the maneuver. The F and G matrices for this case are partitions of Eq. (10), and are shown in Eq. (12). In these cases, the model used to generate the control assumes that there is no modal damping. The parameters used are given in Fig. 1, although η_1 is not given there since it can assume any nonzero value and not affect the outcome.

$$\begin{bmatrix} \theta \\ \dot{\theta} \\ q_1 \\ \dot{q}_1 \end{bmatrix} = \begin{bmatrix} 0 & 1 & 0 & 0 \\ 0 & 0 & 0 & 0 \\ 0 & 0 & 0 & 1 \\ 0 & 0 & -\omega_1^2 & 0 \end{bmatrix} \begin{bmatrix} \theta \\ \dot{\theta} \\ q_1 \\ \dot{q}_1 \end{bmatrix} + \begin{bmatrix} 0 \\ 1/J \\ 0 \\ \eta_1 \end{bmatrix} T \tag{12}$$

For this example, we minimize $\int_0^{t_f} T^2 \mathrm{d}t$ subject to Eq. (12) and the boundary conditions (13)

$$\theta(0) = \theta_0, \quad \dot{\theta}(0) = 0, \quad q_1(0) = 0, \quad \dot{q}_1 = 0, \quad \theta(t_f) = 0, \quad \dot{\theta}(t_f) = 0, \quad q_1(t_f) = 0, \quad \dot{q}_1(t_f) = 0 \tag{14}$$

Therefore, $A = 0$ and $B = 1$. The Euler-Lagrange equations, Eq. (4), become for this case,

$$\frac{\mathrm{d}}{\mathrm{d}t}\begin{bmatrix} \theta \\ \dot{\theta} \\ q_1 \\ \dot{q}_1 \\ \lambda_1 \\ \lambda_2 \\ \lambda_3 \\ \lambda_4 \end{bmatrix} = \left[\begin{array}{cccc:cccc} 0 & 1 & 0 & 0 & 0 & 0 & 0 & 0 \\ 0 & 0 & 0 & 0 & 0 & -1/J^2 & 0 & -\eta_1/J \\ 0 & 0 & 0 & 1 & 0 & 0 & 0 & 0 \\ 0 & 0 & -\omega_1^2 & 0 & 0 & -\eta_1/J & 0 & -\eta_1^2 \\ 0 & 0 & 0 & 0 & 0 & 0 & 0 & 0 \\ 0 & 0 & 0 & 0 & -1 & 0 & 0 & 0 \\ 0 & 0 & 0 & 0 & 0 & 0 & 0 & 0 \\ 0 & 0 & 0 & 0 & 0 & 0 & 0 & 0 \end{array}\right] \begin{bmatrix} \theta \\ \dot{\theta} \\ q_1 \\ \dot{q}_1 \\ \lambda_1 \\ \lambda_2 \\ \lambda_3 \\ \lambda_4 \end{bmatrix} \tag{15}$$

$$\begin{bmatrix} \theta(t) \\ \dot{\theta}(t) \\ q_1(t) \\ \dot{q}_1(t) \\ \lambda_1(t) \\ \lambda_2(t) \\ \lambda_3(t) \\ \lambda_4(t) \end{bmatrix} = \left[\begin{array}{c|c} \Phi_{11}(t) & \Phi_{12}(t) \\ \hline 0 & \Phi_{22}(t) \end{array}\right] \begin{bmatrix} \theta(0) \\ \dot{\theta}(0) \\ q_1(0) \\ \dot{q}_1(0) \\ \lambda_1(0) \\ \lambda_2(0) \\ \lambda_3(0) \\ \lambda_4(0) \end{bmatrix} \tag{16}$$

where

$$\Phi_{11}(t) = \begin{bmatrix} 1 & t & 0 & 0 \\ 0 & 1 & 0 & 0 \\ 0 & 0 & \cos\omega_1 t & \dfrac{\sin\omega_1 t}{\omega_1} \\ 0 & 0 & -\omega_1 \sin\omega_1 y & \cos\omega_1 t \end{bmatrix} \qquad \Phi_{22}(t) = \Phi_{11}^T(-t)$$

$$\Phi_{12}(t) = \begin{bmatrix} \dfrac{t^3}{6J^2} & \dfrac{-t^2}{2J^2} & \dfrac{-\eta_1}{(J\omega_1^2)}\left(\dfrac{\sin\omega_1 t}{\omega_1} - t\right) & \dfrac{\eta_1}{J\omega_1^2}(\cos\omega_1 t - 1) \\ \dfrac{t^2}{2J^2} & \dfrac{-t}{J^2} & \dfrac{-\eta_1}{(J\omega_1^2)}(\cos\omega_1 t - 1) & \dfrac{-\eta_1}{J\omega_1}\sin\omega_1 t \\ \dfrac{\eta_1}{(\omega_1^2 J)}\left(t - \dfrac{\sin\omega_1 t}{\omega_1}\right) & \dfrac{-\eta_1}{\omega_1^2 J}(1-\cos\omega_1 t) & -\eta_1^2 t\cos\dfrac{\omega_1 t}{2\omega_1^2} & -\eta_1^2 t\sin\dfrac{\omega_1 t}{2\omega_1} \\ \dfrac{\eta_1}{(\omega_1^2 J)}(1-\cos\omega_1 t) & -\eta_1 \sin\dfrac{\omega_1 t}{\omega_1 J} & \dfrac{-\eta_1^2}{2\omega_1^2}(\cos\omega_1 t - \omega_1 t\sin\omega_1 t) & \dfrac{-\eta_1^2}{2\omega_1}(\sin\omega_1 t + \omega_1 t\cos\omega_1 t) \end{bmatrix}$$

As $\Phi_{12}^{-1}(t_f)$ was obtained using a computer, the result was substituted into Eq. (9), together with elements from Eqs. (12), (14), and (16) to obtain the desired torque profile.

Figure 2 shows the results of a computer simulation for $\theta_0 = 10$ deg (or 0.17 rad) and $t_f = 5$ s. The torque profile is the sum of a straight line, with small components of $\sin\omega_1 t$ and $\cos\omega_1 t$ superimposed. The rigid body moves smoothly from 0 to 10 deg, and the first bending mode q_1 is excited, but stops when the time reaches 5 s. The second and third bending modes, which were uncontrolled, are also shown.

Figure 3 shows computer simulation results for a 10-deg maneuver, when the maneuver time is 0.50 s. Since the period of the first mode is 1 s, the maneuver is being performed in well under the period of the controlled mode. Again, the torque profile is the sum of a straight line and $\sin\omega_1 t$ and $\cos\omega_1 t$, but this time the contribution from the trigonometric terms is much higher. The rigid-body angle goes through some large changes as more effort is devoted to controlling the first bending mode as well as the rigid-body angle but ends up at the desired 10 deg, and the first bending mode is left quiescent at the end of the maneuver. Also, the effect of this maneuver on the second and third bending modes is shown.

As the model grows beyond one mode, analytical determination of the transition matrix in Eq. (7) becomes increasingly tedious. Therefore, before giving the example for controlling two modes, we show a numerical method for determining the transition matrix.

First, we rewrite Eq. (4) as follows:

$$\begin{bmatrix} \dot{x} \\ \dot{\lambda} \end{bmatrix} = \mathfrak{F} \begin{bmatrix} x \\ \lambda \end{bmatrix} \tag{17}$$

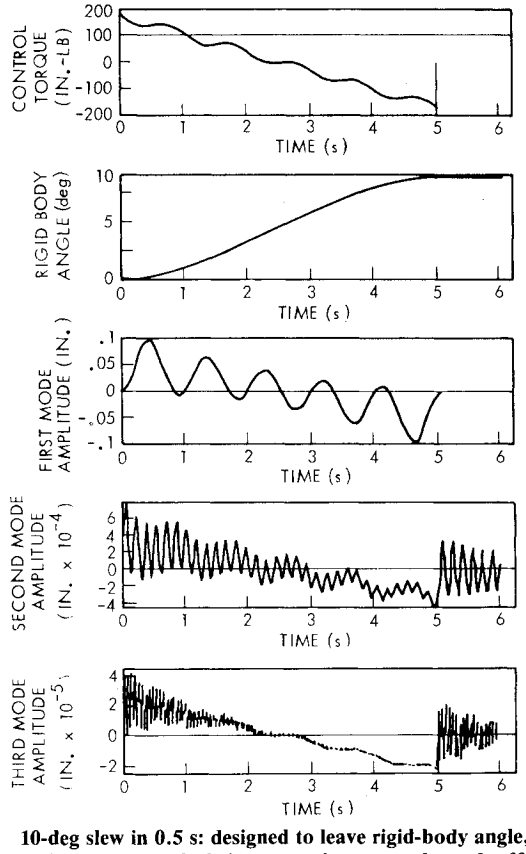

Fig. 2 10-deg slew in 0.5 s: designed to leave rigid-body angle, first-mode amplitude, and both their rates quiescent at the end; effect on next two bending modes also shown.

From Eq. (17) we wish to derive Φ in Eq. (18):

$$\begin{bmatrix} x(t) \\ \lambda(t) \end{bmatrix} = \Phi(t) \begin{bmatrix} x(0) \\ \lambda(0) \end{bmatrix} \tag{18}$$

If $\mathfrak{F}$ has no repeated eigenvalues, its eigenvectors are all linearly independent. In this case, if we call E the matrix made up columnwise of the eigenvectors, E^{-1} exists, and the following decomposition can be performed. Let Λ be the diagonal matrix made up of the eigenvalues of $\mathfrak{F}$; then, if we order the eigenvectors in E correctly,

$$\mathfrak{F}E = E\Lambda \tag{19}$$

We then define a new vector y, twice the length of x, by

$$y = E^{-1} \begin{bmatrix} x \\ \lambda \end{bmatrix} \tag{20}$$

Using Eq. (20) in Eq. (17), the result is

$$E\dot{y} = \mathfrak{F}Ey \tag{21}$$

From Eq. (19), and the postulated existence of E^{-1}, we obtain

$$E^{-1}E\dot{y} = E^{-1}E\Lambda y = \dot{y} = \Lambda y \tag{22}$$

Since Λ is diagonal, the second half of Eq. (22) is readily integrated to give

$$y_i(t) = e^{\lambda_i t} y_i(0) \tag{23}$$

where y_i are the scalar components of the vector y. If we define

$$e^{\Lambda t} \triangleq \begin{bmatrix} e^{\lambda_1 t} & & 0 \\ & e^{\lambda_2 t} & \\ 0 & & \ddots \; e^{\lambda_n t} \end{bmatrix} \tag{24}$$

then

$$y(t) = e^{\Lambda t} y(0) \tag{25}$$

Substituting for y in Eq. (25) by using Eq. (20), we have

$$\begin{bmatrix} x(t) \\ \lambda(t) \end{bmatrix} = Ee^{\Lambda t}E^{-1} \begin{bmatrix} x(0) \\ \lambda(0) \end{bmatrix} \tag{26}$$

Comparison of Eq. (26) with Eq. (18) shows that we have found the desired transition matrix,

$$\Phi(t) = Ee^{\Lambda t}E^{-1} \tag{27}$$

The above derivation of Φ depends on the existence of E^{-1}, which is dependent on the eigenvalues of $\mathfrak{F}$ being distinct. Without proof, we submit that in the case of flexible dynamic systems, this can be made to happen in two ways. The first is that the original F matrix has distinct eigenvalues that are at least a little damped, i.e., they lie to the left of the imaginary axis. For the bending model, this is a realistic assumption. However, adding damping to the rigid-body angle θ is something of a fiction, though if the damping is small enough, perhaps a harmless fiction. The other way of ensuring distinct eigenvalues for $\mathfrak{F}$ is through artful use of the state weighting matrix A, which we have set equal to zero in the previous examples. In addition to allowing the numerical determination of Φ, this latter alternative has the advantage of limiting the excursions of the modal amplitudes during the maneuver. But problems with the HQR2 eigenvalue routine prevented this alternative. We will say more about this in the

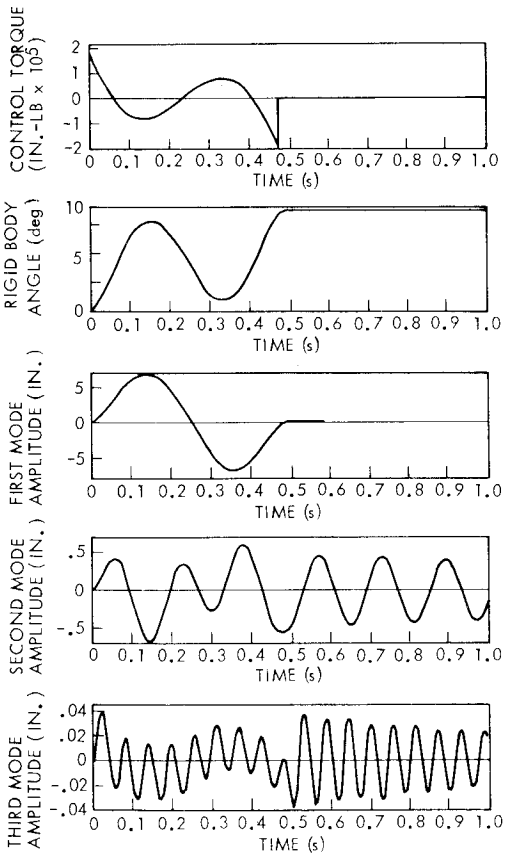

Fig. 3 10-deg slew in 0.5 s: designed to leave rigid-body angle, first-mode amplitude, and both their rates quiescent at the end; effect on next two bending modes also shown.

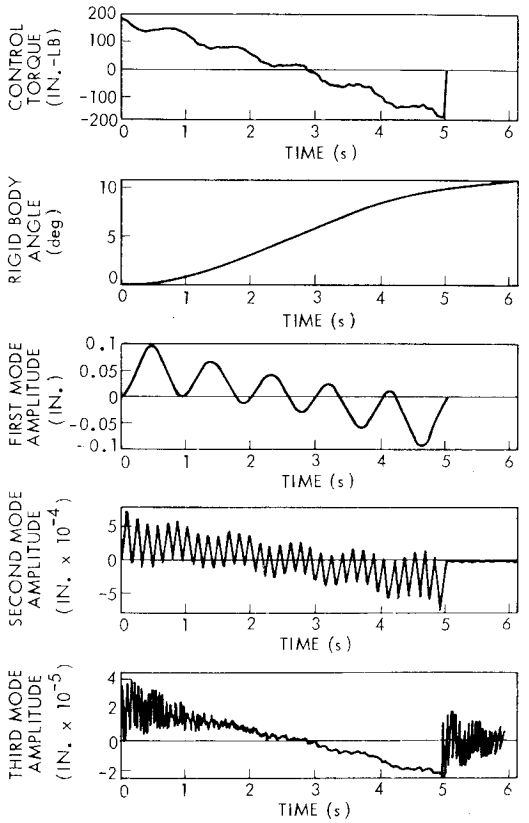

Fig. 4 10-deg slew in 0.5 s: designed to leave rigid-body angle, first two modal amplitudes, and all their rates quiescent at the end; effect on third bending mode also shown.

conclusion. A last advantage of this numerical transition matrix scheme is that it is not necessary to invert E numerically to obtain E^{-1}. If we partition E into its four quadrants,

$$E=\begin{bmatrix} E_{11} & E_{12} \\ E_{21} & E_{22} \end{bmatrix}$$

it is a useful property of the Euler-Lagrange equations, that with proper normalization of the eigenvectors,

$$E^{-1}=\begin{bmatrix} E_{22}^T & -E_{12}^T \\ -E_{21}^T & E_{11}^T \end{bmatrix} \tag{28}$$

In the next example, by adding damping to the original dynamic system (F matrix), we are able to generate an example which uses this numerical transition matrix method to generate a control which leaves two modes inactive at the end of a specified rigid body slew. The modified dynamical system is shown as

$$\frac{\mathrm{d}}{\mathrm{d}t}\begin{bmatrix} \theta \\ \dot\theta \\ q_1 \\ \dot q_1 \\ q_2 \\ \dot q_2 \end{bmatrix}=\begin{bmatrix} 0 & 1 & 0 & 0 & 0 & 0 \\ .001 & .001 & 0 & 0 & 0 & 0 \\ 0 & 0 & 0 & 1 & 0 & 0 \\ 0 & 0 & -\omega_1^2 & -2\zeta_1\omega_1 & 0 & 0 \\ 0 & 0 & 0 & 0 & 0 & 1 \\ 0 & 0 & 0 & 0 & -\omega_2^2 & -2\zeta_2\omega_2 \end{bmatrix}\begin{bmatrix} \theta \\ \dot\theta \\ q_1 \\ \dot q_1 \\ q_2 \\ \dot q_2 \end{bmatrix}+\begin{bmatrix} 0 \\ 1/J \\ 0 \\ \eta_1 \\ 0 \\ \eta_2 \end{bmatrix}T \tag{29}$$

The parameter values are given in Fig. 1. This technique generates the same control profile regardless of the values of η_1 and η_2, as long as they are nonzero. Figures 4 and 5 show the results of a computer simulation driven by this torque. In the case shown by Fig. 4, the time for the maneuver was 5 s and the amount of slew was 10 deg. In Fig. 5 we show the results of a 10 deg, 0.5-s slew. In both cases, the first and second modal amplitudes are almost quiescent at the end of the maneuver. The behavior of the third mode for both slews is also shown.

III. Feedback Slewing

An attractive feature of optimal slewing is that it can be converted easily to a feedback control scheme. This is not meant to imply a constant-gain feedback which causes the state vector to follow some predetermined trajectory, but rather feedback using a time-varying feedback gain which effectively reoptimizes the trajectory at each point in time and causes the desired final conditions to be met at the end of the trajectory.

Consider Eq. (9) for the optimal open-loop torque $u(t)$. This expression is valid for arbitrary initial state $x(0)$. If we pick a new starting time t_1, where $0\le t_1\le t_f$,

$$u(t)=-B^{-1}G^T[\Phi_{21}(t)-\Phi_{22}(t)\Phi_{12}^{-1}(t_f)\Phi_{11}(t_f)]x(t_1) \qquad (t_1\le t\le t_f) \tag{30}$$

Bellman's principle of optimality (see, for example, Ref. 1) assures us that the expression for u in Eq. (30) will be the same as that of Eq. (9) during the interval $t_1\le t\le t_f$, as long as $x(t_1)$ lies on the original trajectory driven by Eq. (9). In particular,

$$u(t)=-B^{-1}G^T[\Phi_{21}(0)-\Phi_{22}(0)\Phi_{12}^{-1}(t_f)\Phi_{11}(t_f)]x(0) \tag{31}$$

or, since $\Phi_{21}(0)=0$ and $\Phi_{22}(0)=I$

$$u(0)=B^{-1}G^T\Phi_{12}^{-1}(t_f)\Phi_{11}(t_f)x(0) \tag{32}$$

But, since time zero is arbitrary, let $t'=t_f-t$. Thus, t' is the time to go. Now,

$$u(t)=B^{-1}G^T\Phi_{12}^{-1}(t')\Phi_{11}(t')x(t) \tag{33}$$

the coefficient of $x(t)$ can be considered a set of time-varying gains, independent of the initial conditions $x(t)$, which make $x(t')=0$.

This time-varying gain matrix considers the state of any time t, and determines u which will be given the optimal trajectory into the point $x=0$ at the end of the maneuver.

However, there is one problem. As the time to go t' goes to zero, Φ_{12} also goes to zero. This means that Φ_{12}^{-1} is singular at the end of the maneuver. Although it is ideally true that x goes to zero at the same time in such a way the product $\Phi_{12}^{-1}x$ stays finite, this is still not a practical gain. To overcome this problem, we reformulate the original problem. Now we choose to minimize Eq. (34) by choice of u, subject to the

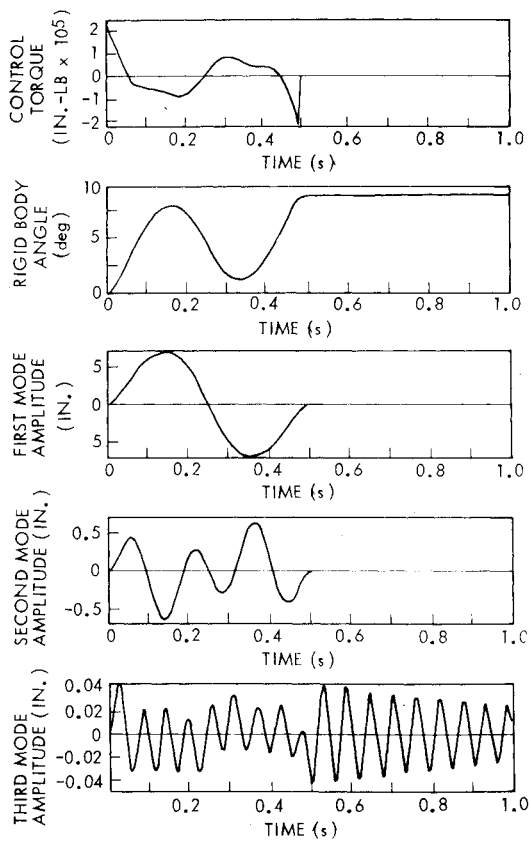

Fig. 5 10-deg slew in 0.5 s: designed to leave rigid-body angle, first two modal amplitudes, and all their rates quiescent at the end; effect on third bending mode also shown.

constraints in Eq. (35) and the boundary condition in Eq. (36):

$$x^T(t_f)S_f x(t_f) + \int_0^{t_f} (x^T Ax + u^T Bu)\,dt \tag{34}$$

$$\dot{x} = Fx + Gu \tag{35}$$

$$x(0) \quad \text{given} \tag{36}$$

Instead of demanding that $x(t_f)$ be exactly zero, we simply weight $x(t_f)$ in the cost function with the weighting matrix S_f. This new problem has the same Euler-Lagrange Eq. (4), and Eq. (5) still holds. But the boundary conditions in Eq. (6) are changed to

$$x(0) \quad \text{given} \quad \lambda(t_f) = S_f x(t_f) \tag{37}$$

The change in the boundary conditions has no effect on the transition matrix $\Phi(t)$ of the Euler-Lagrange equations, so we can use methods of Sec. II to get the control u. It turns out that the answer is

$$u(t) = -BG^T[\Phi_{21}(t) + \Phi_{22}(t)S_f^{-1}\Phi_{22}(t_f) - \Phi_{12}(t_f)]^{-1}$$
$$\times [\Phi_{11}(t_f) - S_f^{-1}\Phi_{21}(t_f)]x(0) \tag{38}$$

Note that as we raise the weight on $x(t_f)$ but letting $S_f \to \infty$, expression (38) becomes the same as Eq. (9).

Now, using the same reasoning as that in the beginning of this section and making the same substitutions that were used to obtain Eq. (33), we get the feedback from

$$u(t) = -B^{-1}G^T[S_f^{-1}\Phi_{22}(t') - \Phi_{12}(t')]^{-1}$$
$$\times [\Phi_{11}(t') - S_f^{-1}\Phi_{21}(t')]x(t) \tag{39}$$

The gain part of expression (39) now remains finite at $t' \to 0$.

The storage of these gains in an onboard computer could constitute a problem. A gain is needed for each state to be controlled, and for each state the gains must be stored to

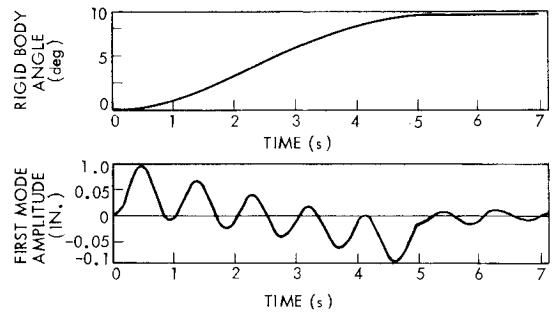

a) First-mode frequency contains 1% error.

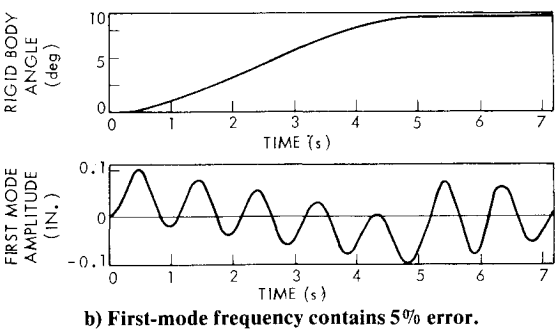

b) First-mode frequency contains 5% error.

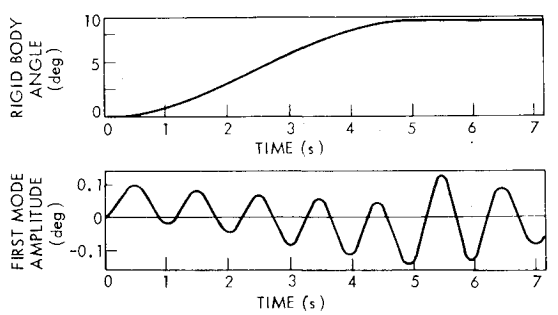

c) First-mode frequency contains 10% error.

Fig. 6 10-deg slew in 5 s, open-loop torque designed to eliminate first mode at end.

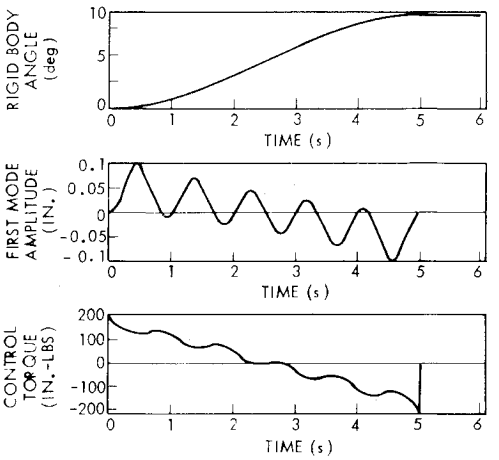

a) First-mode frequency contains 1% error.

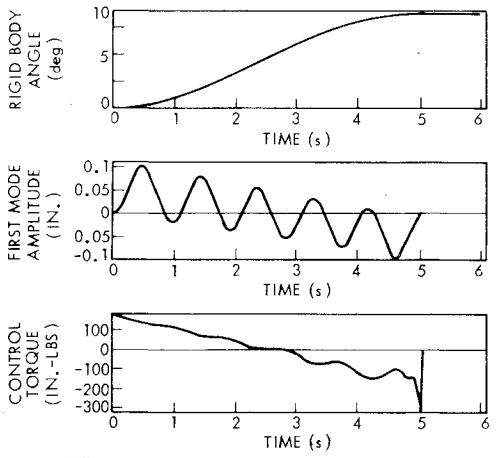

b) First-mode frequency contains 5% error.

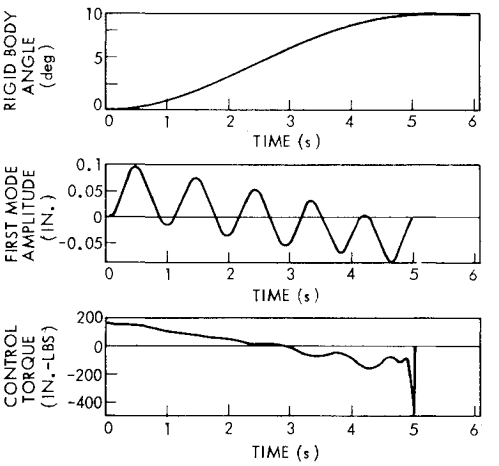

c) First-mode frequency contains 10% error.

Fig. 7 10-day slew in 5 s, feedback torque designed to drive first mode to zero at end.

cover, with reasonable granularity, the time during which maneuvers are to be performed. However, since the gains are independent of $x(t)$, they are independent of the maneuver desired. More concisely, one set of gains can do any maneuver. To do the maneuver, just add a constant vector to the state vector, so that the desired state at time t_f becomes zero, then apply the gains to this modified state vector.

If the weight S_f is chosen large enough, the open-loop control and the feedback control behave the same, as long as there are no parameter errors. In the presence of parameter error, however, the added difficulty in implementing the feedback scheme is well rewarded. To fully appreciate the advantage of the feedback method, it is necessary to examine the misbehavior of the open-loop method in the presence of parameter errors. If the model used to generate the open-loop torques used the wrong frequency, one would expect some degradation of performance, i.e., the end conditions would not be met exactly. Figure 6 shows the same maneuver as shown in Fig. 2, except the model uses the wrong frequency for the first bending mode.

In Fig. 6a the error in the frequency is 1%, in Fig. 6b it is 5%, and in Fig. 6c it is 10%. The residual error in the first bending mode amplitude grows quickly as the frequency error goes up. For a moderate error of 10%, the residual amplitude is larger than any of the excursions during the maneuver! Compare these results with Fig. 7 which shows how the feedback control behaves with the same errors in the frequency parameter. The performance is similar to the open-loop control until just before the end of the maneuver, when the feedback method insists on bringing the bending mode to an inactive state.

Finally, a simple alternative to the optimal fixed-time feedback slew is presented. If extremely good performance is not necessary, it may be possible to get by with using a constant gain approach. Figure 8 shows the histories of the first and rigid modes and the control for just such a case. Constant gains are generated for the rigid-body angle, the first bending mode, and both of their rates. The rigid-body angle is then offset by ± 0 deg and the controller is turned on. The result is a 10-deg slew which is fairly well completed within 5 s. The simplicity of this approach makes it an attractive alternative to the more complicated methods which have been the subject of earlier sections. The constant gains used for the maneuver shown in Fig. 8 were generated by standard optimal control techniques. The rigid-body angle and the first mode were weighted proportionately to their contribution to a displacement of the tip of one of the flexible beams. (Their rates were not weighted.) The weight on the control was then varied until the first mode was critically damped.

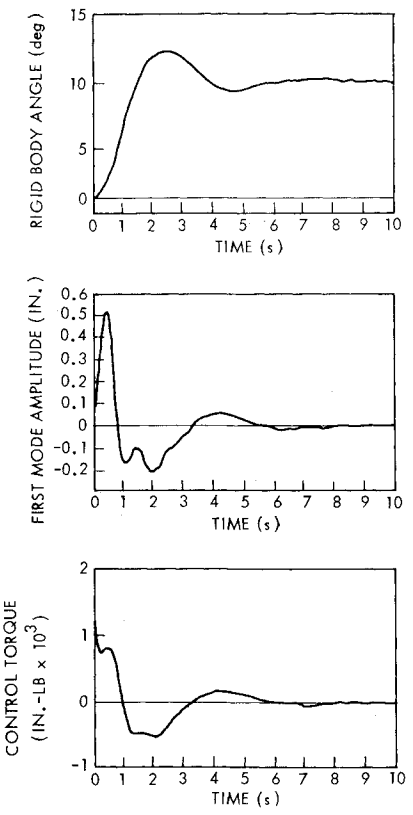

Fig. 8 Constant-gain 10-deg slew.

IV. Experimental Verification

The Modal Lab at Lockheed Missiles & Space Company has built a physical specimen very much like the example shown in Fig. 1. This specimen was used to test the open-loop slewing theories decribed in Sec. II.

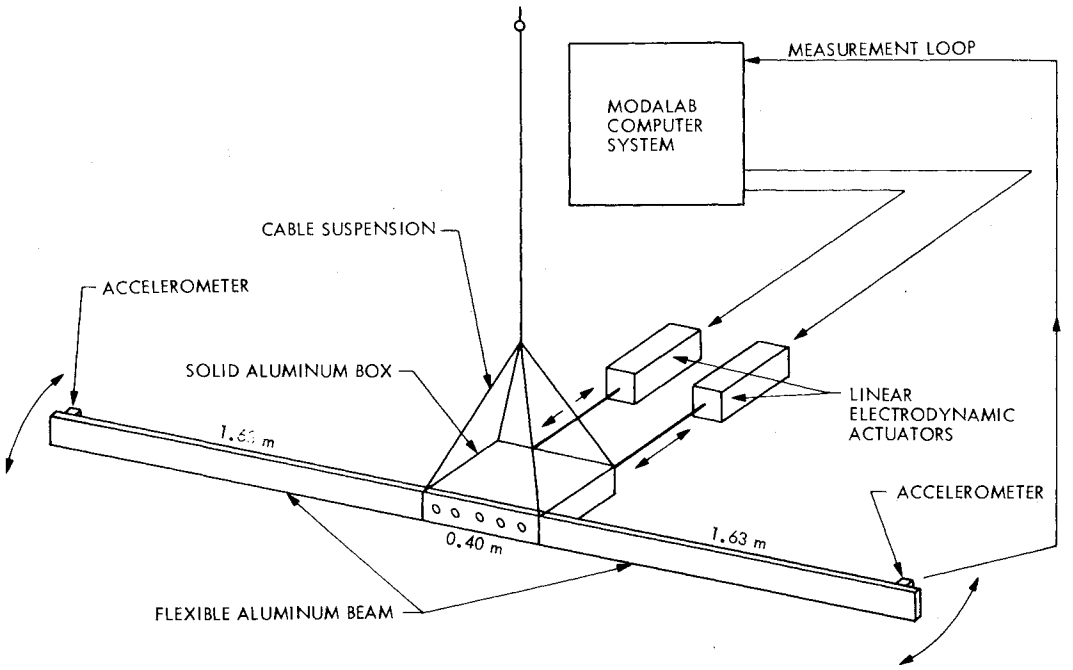

Fig. 9 Drawing of experimental vehicle.

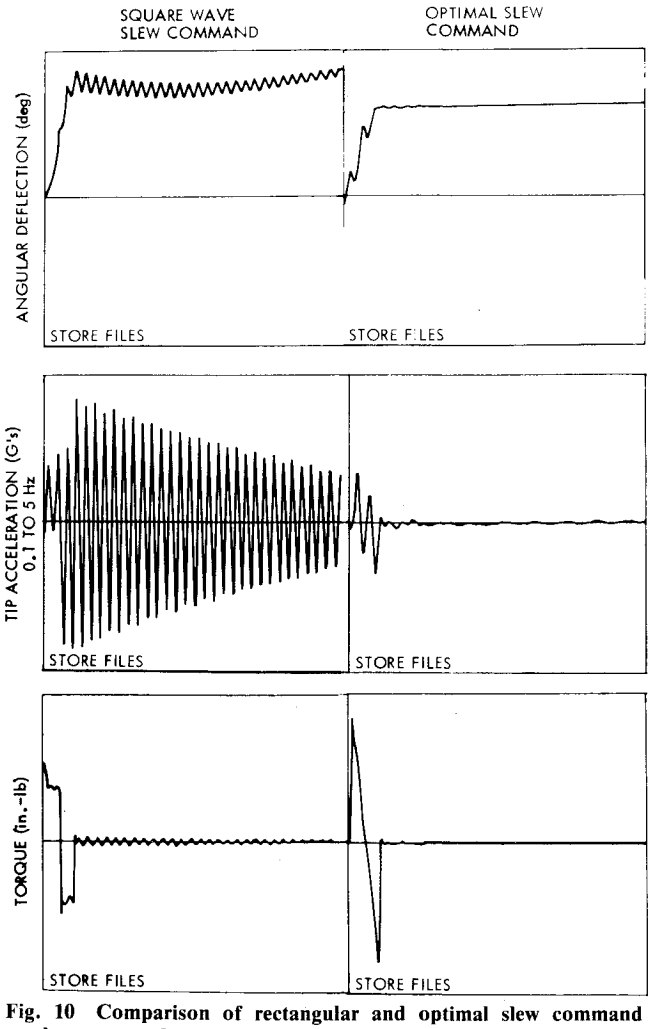

Fig. 10 Comparison of rectangular and optimal slew command results, command period = 1.0 s.

A drawing of the test specimen is shown in Fig. 9. The specimen consists of a rigid block of aluminum in the middle, with a long flexible bar of aluminum attached to each side. The central block is suspended from the ceiling by thin wires. The control is provided by two Electroseis linear actuators which act on the rigid central body. For these experiments, the linear actuators are commanded to give equal but opposite forces, resulting in a pure torque on the rigid central body. There are two sets of sensors installed. On both ends of the flexible bar, accelerometers provide information on the tip acceleration. Connected in parallel with the Electroseis linear actuators are linear potentiometers which measure the amount of rotation of the central body. Small masses are also attached to each end of the flexible bar so as to lower the frequencies of the natural modes.

The equations of motion for this specimen are the same as those in Eq. (29). However, the parameters in this case are $\omega_1 = 2.62$ Hz, $\omega_2 = 9.4$ Hz, and $J = 135.05$ lb-in.-s^2.

For these experiments, the commands to the linear actuators were provided by a PDP 1145 digital computer. The desired profiles were approximated by small segments of constant output. Each command was divided into 100 such segments. The output from the computer was fed through a digital-to-analog converter, and then smoothed by an eight-pole Butterworth filter set at 100 rad/s before being input to the actuators.

The effectiveness of this slewing technique is demonstrated in Fig. 10. Both slews are through 10 deg. For comparison purposes, the response to square-wave torque commands are also shown. The tip acceleration output is filtered to show frequency content between 0.1 and 5 Hz. The optimal slew shows almost no residuals of the tip accelerations at the end of the maneuvers. What residual there is can be attributed to the 1-Hz symmetric mode, which was not controlled, and only insignificantly excited.

V. Conclusions

We have some further comments on the implementation of the ideas contained in this paper. First, we showed the behavior of the third bending mode under the influence of the various slewing torques in Figs. 2-5. Again from these figures, it is noticed that as more modes are controlled, the unmodeled modes get more excited both during and after the maneuver. This is, of course, undesirable, but there is a solution. A controller which has little high-frequency content could be included in the dynamics of the system. This would prevent any significant excitation of the higher unmodeled modes.

Figures 2-5 show that even though the controlled modes are left quiescent at the end of the maneuver, they undergo large excursions during the maneuver, especially for the quicker maneuvers. This could result in structural damage during the maneuver. The obvious solution is to use state weighting during the maneuver through a nonzero A matrix. Attempts to do this were thwarted by misbehavior of the HQR2 eigenvalue routine. Those values of A which might alleviate the excessive modal excursions caused HQR2 to be unable to find the eigenvalues, much less the eigenvectors of the Euler-Lagrange system. This is mentioned in the hope that others have experienced the same problem and can suggest a solution.

Finally, remember that all the methods suggested in this paper depend on the dynamics matrices F and G being constant in time. Modern numerical methods can easily be used to obtain transition matrices for time-varying systems, and minor modifications of the theories presented herein would permit application to time-varying dynamic systems.

Reference

[1] Bryson, A. and Ho, Y.C., *Applied Optimal Control,* Ginn-Blaisdell, Waltham, Mass., 1969, p. 148.